



**UNIVERSITY  
OF TURKU**

This is a self-archived – parallel published version of an original article. This version may differ from the original in pagination and typographic details. When using please cite the original.

This version of the article has been accepted for publication, after peer review (when applicable) and is subject to Springer Nature's [AM terms of use](#), but is not the Version of Record and does not reflect post-acceptance improvements, or any corrections. The Version of Record is available online at:

DOI <https://doi.org/10.1007/s10569-021-10050-8>

ARTICLE  
INFORMATION/  
CITATION

Tanikawa, K., Mikkola, S. Numerical confirmation of the existence of triple collision orbits inside the domain of the free-fall three-body problem. *Celest Mech Dyn Astr* **133**, 52 (2021). <https://doi.org/10.1007/s10569-021-10050-8>

# Numerical confirmation of the existence of triple collision orbits inside the domain of the free-fall three-body problem

Kiyotaka TANIKAWA · Seppo MIKKOLA

Received: June 27, 2021 / Accepted: date

**Abstract** We performed numerical orbit integrations of the equal-mass free-fall three-body problem. We provided numerical evidence of the existence of triple collision orbits concentrating on the shape of triangles formed by the three bodies. In the process, in the negative side, we confirmed that the shape of the triangle of non-triple collision orbits deviates from equilateral as the orbit approaches the instant of supposed triple collision. In the positive side, the orbit integrations have been done along the three binary collision curves on which the orbit perform binary collision. These curves meet at the triple collision point (TCP). Three binary collisions have the three base edges, whose direction define the edges of the triple collision orbit. The triangle defined by these three edges precisely coincides with the equilateral triangles of the triple collision orbit.

**Keywords** Three-body problem · Triple collision · Free-fall problem

**Mathematics Subject Classification (2020)** MSC code1 · MSC code2 · more

---

F. Author  
National Astronomical Observatory of Japan, Mitaka, Tokyo, 181-8588 Japan  
Tel.: +81-422-34-3605  
E-mail: Tanikawa.ky@nao.ac.jp

S. Author  
Tuorla Observatory, Department of Physics and Astronomy, University of Turku, FI-20014  
Turku, Finland

## 1 Introduction

### 1.1 Motivation and setting

We have obtained eleven simplest triple collision orbits in the free-fall three-body problem (Tanikawa, Saito, and Mikkola 2019; hereafter referred to as Paper I). Here, by ‘simplest’ orbits we mean those having shortest orbital arcs in the sense of symbol sequences.

Sergei Klioner raised a doubt, “The orbits you have obtained may not be true triple collision orbits. If you integrate orbits with more accuracy, you may obtain non-collision orbits.” Then, we felt a necessity of some kind of numerical evidence so that Sergei may be convinced though we were confident of our results. We started a project. The purpose is threefold. We will talk about the project after the explanation of the setting of the problem.

We consider as in Paper I the free-fall three-body problem. Let  $m_i$  be the mass of the  $i$ th body. Let  $t$  be the time and  $\mathbf{r}_i$  be the positions of body  $m_i$  at  $t$ . Let  $\mathbf{r}_{ij}$  be the position vector from body  $m_j$  to body  $m_i$ . The equations of motion are

$$\frac{d^2\mathbf{r}_i}{dt^2} = -\sum_{j \neq i} \frac{m_j \mathbf{r}_{ij}}{|\mathbf{r}_{ij}|^3}, \quad i = 1, 2, 3 \quad (1)$$

We put bodies  $m_2$  and  $m_3$ , respectively, at  $A(-0.5, 0)$  and  $B(0.5, 0)$  in the  $(x, y)$  plane, and put body  $m_1$  at any place  $P$  in the region

$$D = \{(x, y) : ((x + 0.5)^2 + y^2) \leq 1, x \geq 0, y \geq 0\} \quad (2)$$

We assume  $m_1 = m_2 = m_3 = 1$ . We start the motion of the three bodies with zero velocities. Thus we have the name ‘the (equal mass) free-fall three-body problem’. We call region  $D$  the initial condition region or plane (see Fig. 1). In the figure,  $\Gamma_1$  (segment  $EB$ ) represents the initial conditions for collinear three-body problem, whereas  $\Gamma_2$  (segment  $EC$ ), and  $\Gamma_3$  (circular arc  $BC$ ) represent the isosceles three-body problem.

In Paper I, we introduced symbols and symbol sequences in such a way that each time the three bodies become collinear (syzygy), we gave symbol 1, 2 or 3 according to which body is in between the remaining two bodies, and that we represented the sequence of syzygies by a sequence of symbol 1, 2 or 3 which replaces the continuous trajectory described in the phase space. We consider the future symbol sequences starting at the free-fall state. Any point of the initial condition plane  $D$  in Fig. 1 has symbol sequences other than the equilateral point  $C$  whose orbit does not experience syzygy (Montgomery, 2007). Symbol sequences of the orbits starting at three boundaries  $\Gamma_i, i = 1, 2, 3$  are degenerate in the sense that the central body is fixed in every syzygy. Triple collisions on  $\Gamma_1$  and  $\Gamma_3$  have been discussed in Tanikawa & Mikkola (2015). Triple collisions of  $\Gamma_2$  will be discussed elsewhere.

Symbol sequences truncated at some digit, say at  $k > 0$ , constitute a set of symbol sequences. We call this the  $k$ -cylinder set, or simply the  $k$ -cylinder.

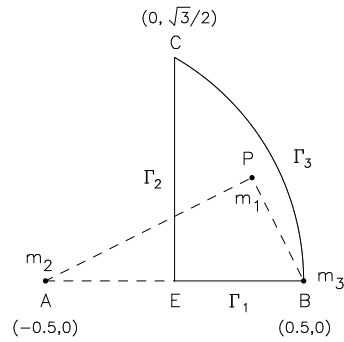


**Fig. 1** Geometry of the free-fall three-body problem.

The initial positions of a  $k$ -cylinder occupy a set of points in  $D$ . By abuse of words, we call this set of the initial condition plane also the  $k$ -cylinder (set). Given a  $k > 0$ , the initial condition plane  $D$  is divided by the set of all  $k$ -cylinders. Positive integer  $k$  is called a generation (see §4.1 of Tanikawa et al. 2019 for the definition of 'generations').

We have shown in Paper I that for a fixed  $k > 0$  the boundaries of adjacent  $k$ -cylinders are formed with binary collision curves (BCCs), that is, the curves of initial conditions such that the orbits starting there experience binary collision. It is to be noted that there are three types of BCCs. The binary collision between body 1 and 2 is said to be of type 3, between bodies 2 and 3 of type 1, and between bodies 1 and 3 of type 2. One of the main results of Paper I has been that the triple collision point (TCP) is obtained as a crosspoint of three BCCs of different types of the same generation.

## 1.2 Purpose

Now we can talk about our purpose. We want to show numerically that the triple collision orbits which we obtained will really experience triple collision. Though our procedures to find triple collision orbits use numerical integrations, these are based on theoretical consideration. More precisely, orbits necessarily have syzygy sequences which are translated into symbol sequences, the initial condition plane is divided into different cylinders, boundaries of cylinders are curves of initial conditions of BCCs, and a TCP is obtained as an intersection of three BCCs of the same generation and of the three different types.

We consider that the following three independent numerical integrations of orbit give strong evidence that our TCPs are not the numerical artifact.

- (1) Suppose we approach one of the TCPs along the three BCCs converging at it. The shape of the triangles formed by three bodies on the binary collision orbits is isosceles at binary collision. The direction of the base of

the isosceles triangles tends to some definite value if the initial conditions of the orbits approach the TCP.

- (2) We want to show that the shape of the triangle formed by the three bodies on our triple collision orbit tends toward equilateral as the orbit approaches the final collision.
- (3) We take a few representative sequences of points tending to TCP from arbitrary directions other than along BCCs. We want to show that the shape of the triangles formed by the three bodies on the orbits along this sequence does not converge at the equilateral shape.

The third item shows that if we approach a TCP from arbitrary directions other than along BCCs, the triangles formed by the three bodies deviate from the equilateral one before the instant of triple collision of our TCO (triple collision orbit) though the deviation starts closer to the final instant if the initial positions become closer to those of the TCP.

The second item shows that the triangle formed by the three bodies on our triple collision orbit approach the equilateral one. In addition, the orientation of the triangle has a definite direction. Of course, we are afraid that the shape may deviate from the equilateral one at extremely close instant of triple collision if ours are not the true collision orbit.

We will confirm that the orientations of the limiting triangles from items (1) and (2) coincide. Then ours are really the triple collision orbit because, three directions along three BCCs differ by  $120^\circ$ , implying that three bases form the equilateral triangle and the orientations of the equilateral triangle are the same as obtained in the second item.

Numerical orbit integrations have been carried out using the code with Algorithmic regularization (Mikkola & Tanikawa 1999, 2013). Symbols sequences have been obtained together.

## 2 Orbits on the binary collision curves

It is well-known that triple collision singularity is replaced by the triple collision manifold which can be smoothly approached by actual orbits (McGehee, 1974). This replacement has been realized by the coordinate changes and time transformation. In particular due to this time transformation, it takes an infinite time for the orbit to arrive at triple collision singularity. Triple collision orbits are on the stable manifold of this triple collision manifold (for the isosceles three-body problem, see, e.g., Devaney, 1980; Simó & Martinez, 1988. For the general planar three-body problem, see, e.g., Moeckel, 1989, Xia, 1992). The stable manifold to the triple collision manifold contains the triple collision orbits of equilateral type and those of collinear type.

In our case, the three bodies on the triple collision orbit near the triple collision form a triangle close to the equilateral one. If we fix a triple collision, the direction of the edges of the triangle is expected to tend to a definite value. We know that three BCCs meet at a TCP. If binary collisions take place,

**Table 1** Approach to TCP at (0.19208270, 0.30936018) along BCCs. 'Angle' is the direction angle of motion of the body 1, 2, or 3 before the final syzygy.

Positions on a BCC				
$x$	$y$	Time	Angle	Round values
Body 1 is slingshot				
0.19209000	0.30936650	1.3545	125.70	
0.19212000	0.30939050	1.3546	125.72	126.0
0.19240000	0.30961500	1.3548	126.10	
Body 2 is slingshot				
0.19205000	0.30932700	1.3543	6.02	
0.19190000	0.30916500	1.3546	5.92	6.0
0.19160000	0.30884700	1.3546	5.92	
Body 3 is slingshot				
0.19205000	0.30934500	1.3544	245.87	
0.19190000	0.30926500	1.3547	245.34	246.0
0.19160000	0.30909500	1.3548	244.92	

the third body passing through between colliding bodies moves perpendicular to the base edge, which implies the three slingshot paths are rotated by  $120^\circ$  with center at triple collision point. This can be confirmed by numerical integrations.

We have done numerical integrations of orbits starting at points on the three BCCs. Three points along each BCC are selected so that the distances between the points and the TCP decrease in succession. The numerical experiments have been done for eleven TCPs. However, we list only the result for the TCP at (0.19208270, 0.30936018) in Table 1. We omitted the remaining results for the brevity of description. Table 1 is arranged so that the first and second columns are the coordinates of the starting position along the three BCCs. The third column represents the time just before the passing of the third body through the center of the remaining two bodies <sup>1</sup>. We list the direction in degrees of motion of the third body in the fourth column. The fifth column stands for the round value of the values in the fourth column. In the table, round values are  $126^\circ.0$ ,  $6^\circ.0$ , and  $246^\circ$  which happen to differ  $120^\circ$  each other.

We summarize the final results of orbit integrations along BCCs for eleven TCPs in Table 2. The first column represents the serial number of TCPs. The second and third columns show the coordinates in the initial condition region of the TCP. The fourth through sixth columns stand for the directions of motion of the slingshot bodies 1, 2, and 3 at around the binary collision. These values are round and taken from the results of orbit integrations along BCCs converging at eleven TCPs. The seventh through ninth columns show the corresponding directions of the base edges. One sees 2-3 in the seventh column of the fifth row (the first to fourth rows are the explanations of the respective columns). The angle is  $36^\circ.0$ . The order of 2-3 has a meaning. The

<sup>1</sup> This is the slingshot effect that the third boy is accelerated or decelerated when it passes through between the remaining two bodies

**Table 2** The directions of motion of the bodies toward triple collision, and the shape and orientation of the equilateral triangle formed by three bodies at triple collision.

	x	y	Directions of motion of the bodies			Directions of edges			Front or back
			1	2	3	2-3	1-3	1-2	
1	0.19208270	0.30936018	126.0	6.0	246.0	2-3 36.0	1-3 96.0	2-1 336.0	back
2	0.22202750	0.30096440	171.0	51.0	291.0	2-3 81.0	1-3 141.0	2-1 21.0	back
3	0.10677930	0.52012268	341.0	221.0	101.0	3-2 71.0	1-3 311.0	1-2 11.0	back
4	0.08875296	0.45639865	351.0	231.0	111.0	3-2 81.0	1-3 321.0	1-2 21.0	back
5	0.15567083	0.33309483	77.0	317.0	197.0	3-2 167.0	1-3 47.0	1-2 107.0	back
6	0.15882908	0.64735217	27.0	147.0	267.0	2-3 117.0	1-3 57.0	1-2 357.0	front
7	0.08212247	0.41682453	1.0	241.0	121.0	3-2 91.0	1-3 331.0	1-2 31.0	back
8	0.27949737	0.57593177	262.0	22.0	142.0	2-3 352.0	3-1 112.0	2-1 52.0	front
9	0.19095011	0.58286178	195.0	315.0	75.0	3-2 105.0	3-1 45.0	1-2 165.0	front
10	0.09012264	0.38213664	17.0	257.0	137.0	3-2 107.0	1-3 347.0	1-2 47.0	back
11	0.10106723	0.37459122	26.0	266.0	146.0	3-2 116.0	1-3 356.0	1-2 56.0	back

angle is measured for the edge 2-3 starting at body 2 to body 3 with respect to the positive  $x$ -axis. Similarly in the eighth column, angle  $96^\circ.0$  is measured for edge 1-3 starting at body 1 to body 3, while in the ninth column, angle  $336^\circ$  is measured at body 2 to body 1. The tenth column shows the side, front or back, of the triangle. We say that the triangle formed by bodies 1, 2, and 3 is of front side if the three bodies are arranged counter-clockwise with respect to the gravity center, while of back side if they are arranged clockwise.

As we pointed above, the directions of the three edges are of round values. We adjusted the values within  $\pm 1^\circ$  from the calculated values. These adjustments bring three angles to fit in with those of the equilateral triangle (see §3).

### 3 The shape and orientation of the triangles toward triple collision

According to Moeckel (1989), the equilateral and collinear fixed points on the triple collision manifold have fixed stabilities for a large open set of mass ratios including the equal mass case. Then, we cannot characterize eleven TCPs by difference of stability. One apparent feature of triple collision is the direction

of edges of the equilateral triangle in the plane. The difference of the direction of the initial and final triangles characterizes different triple collision orbits.

In this section, we numerically integrate the (approximate) triple collision orbits which we have obtained in the preceding work (Tanikawa et al. 2019), and confirm the shape of the triangle and its orientation in the  $(x, y)$ -plane. We measure the shape of the triangles at three instants. The first is at  $t = 0$ , i.e., the initial triangle. Both the second and third instants are close to the instant of triple collision. We confirm that the shape of the triangles at the second and third instants are both close to equilateral.

The numerical results of eleven initial positions are listed in Table 3. In the table, the coordinates of body  $m_1$  in the  $(x, y)$ -plane are listed in the first two columns. The third column represents the instant at which the inner triangle is snapshot. We list the parameters of the triangles in columns 4 through 9 of the table. The fourth column shows the edge of the triangle containing bodies  $m_2$  and  $m_3$ . The fifth column stands for the angle in degrees the orientation of this edge, where 2-3 means that the angle is measured the direction from  $m_2$  to  $m_3$ , whereas 3-2 means that the angle is measured the direction from  $m_3$  to  $m_2$ . The meaning of the sixth and seventh columns are similar, and that of eighth and ninth columns are similar. Three angles of fifth, seventh, and ninth columns together represent the approximate equilateral triangle.

The shapes of the triangles formed by three bodies for eleven triple collision orbits are shown in Figs. 2, 3, and 4. There are three triangles in each row. The left panel shows the initial triangle. Body  $m_2$  and  $m_3$  are at  $(-0.5, 0)$  and  $(0.5, 0)$ . There are two triangles in the right panel of Figs. 2, 3, and 4. These are the triangles in two different instants toward triple collision of the orbit under consideration.

The shapes of the triangle in the right panel almost do not change in the two different instants of time close to triple collision. This indicates that our orbits tend to triple collision in contrast to the results of section 4 in what follows.

As we pointed out in the top of this section, the only parameter which characterizes triple collision is the direction of the equilateral triangle at collision. However, information of this direction is not enough to identify a triple collision orbit because the problem is isotropic and the triangle can be rotated arbitrary. We need both the initial triangle and final equilateral triangle. Thus we show them in Figs. 2, 3, and 4. For the moment, we can say that the number of triple collision orbits is (at least) countable since the number of BCCs is countable and hence the number of their intersections is countable. On the other hand, the number of the relative angles of the initial and final triangles is more than countable. We will talk about this in the last section.

**Table 3** The shape of the triangle just before triple collision

positions		time	edges and angles					
0.19208270	0.30936018	1.35449	2-3	35.7	1-3	95.4	2-1	336.0
0.22202750	0.30096440	1.30830	2-3	80.2	1-3	140.1	2-1	20.2
0.10677930	0.52012268	1.83649	3-2	71.6	1-3	311.3	1-2	11.7
0.08875296	0.45639865	1.99370	3-2	81.9	1-3	321.3	1-2	22.1
0.15567083	0.33309483	1.67785	3-2	167.6	1-3	47.2	1-2	107.9
0.15882908	0.64735217	2.90449	2-3	117.3	1-3	57.4	1-2	357.3
0.08212247	0.41682453	2.16119	3-2	91.2	1-3	330.4	1-2	31.5
0.27949737	0.57593177	3.04699	2-3	352.4	3-1	112.4	2-1	52.6
0.19095011	0.58286178	3.08920	3-2	105.3	3-1	45.4	1-2	165.5
0.09012264	0.38213664	2.30789	3-2	107.8	1-3	346.7	1-2	48.3
0.10106723	0.37459122	2.28150	3-2	116.5	1-3	355.6	1-2	57.0

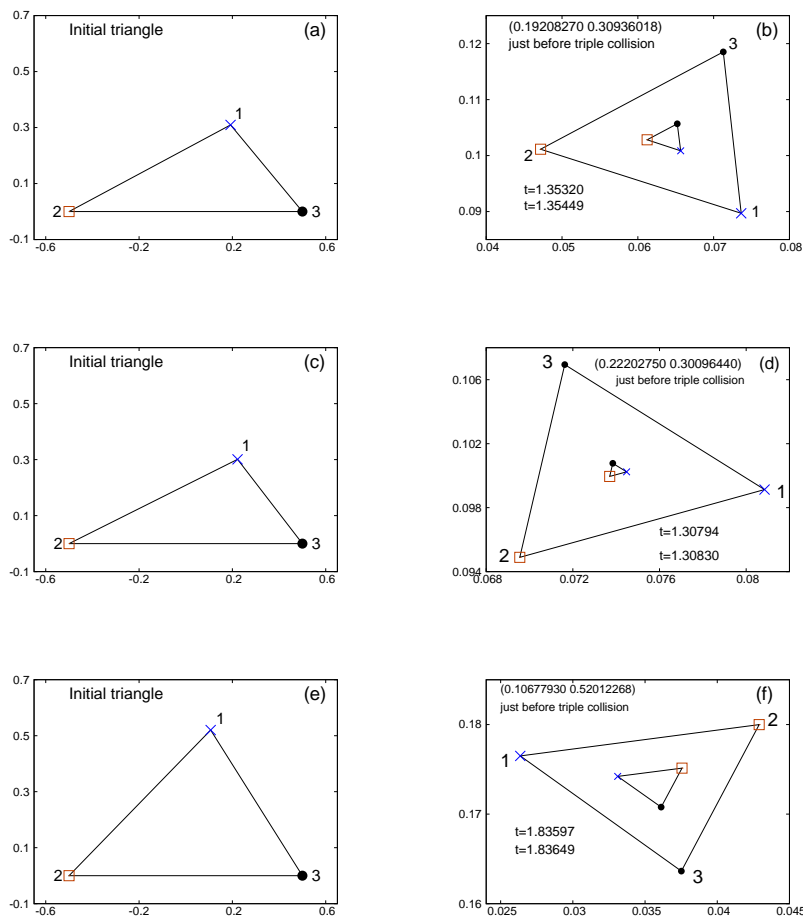


**Fig. 2** The initial (left) and final (right near equilateral) triangles formed by three bodies. Two triangles are superposed in the right panel for different timings. We see the shapes do not change toward triple collision. Orientations are proper to individual triple collisions. Initial conditions are  $(0.10207270, 0.30936018)$ ,  $(0.22202750, 0.30096440)$ , and  $(0.10677930, 0.52012268)$ .

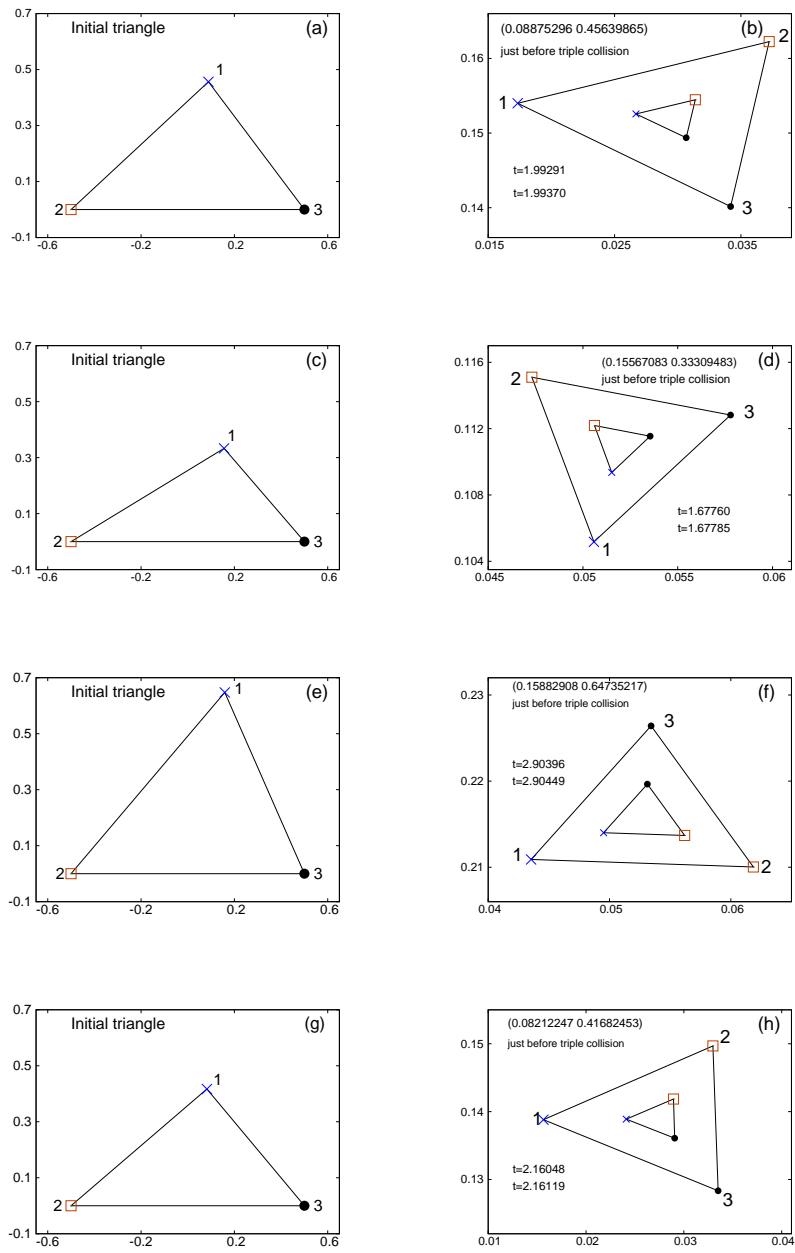


**Fig. 3** (continuation) See the caption of Fig. 2 for the explanations of triangles. Initial conditions are (0.08875296, 0.45639865), (0.15567083, 0.33309483), (0.15882908, 0.64735217), and (0.08212247, 0.41682453).

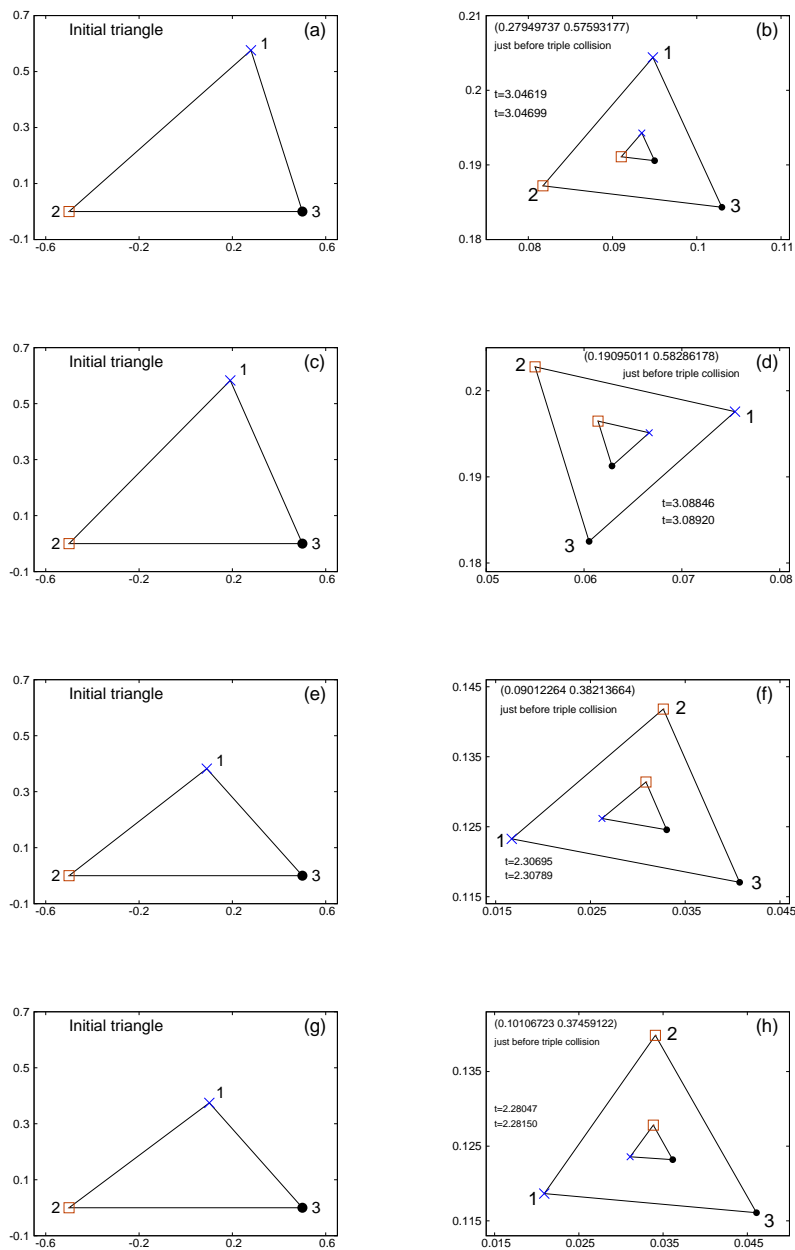


**Fig. 4** (continuation) See Fig. 2 for the explanations of triangles. Initial conditions are (0.27949737, 0.57593177), (0.19095011, 0.58296178), (0.09012264, 0.38213664), and (0.10106723, 0.37459122).

#### 4 The shape of the triangle formed by three bodies off binary collision curves

We confirmed in Section 2 that the shape of the triangles formed by three bodies on the orbits starting at collision curves toward the TCP (triple collision point) becomes isosceles with base of a definite direction. The three types of isosceles triangles define the shape of the limiting triangle of the triple collision orbit starting at the common points of the three collision curves.

In section 3, we confirmed that the triangle formed by the three bodies on the triple collision orbit converges at the equilateral shape. We also confirmed that the directions of equilateral triangles obtained in sections 2 and 3 coincide, which strongly suggests that two kinds of numerical study are reliable.

Theoretically (Devaney 1980; Xia 1992), the trajectories in the phase space of the triple collision orbit should be on the stable manifold of the triple collision manifold. In our words, the form of the triangle approaches equilateral or collinear. We can approach the TCP on our initial condition plane only along the BCCs. This suggests that our triple collisions are equilateral.

Let us quantify the closeness of the shape of the triangle relative to that of the equilateral triangle. We put the triangle in our initial condition plane. Suppose we are given a triangle formed by the three bodies. Let  $a, b$ , and  $c$  with  $1 = a \geq b \geq c \geq 0$  be the lengths of the edges after shrinking or enlarging the triangle until  $a = 1$ . using the cosine formula, we obtain the coordinates of the triangle in our plane as  $x = (a^2 + b^2 - c^2)/(2a) - 0.5$  and  $y$ . The distance  $R$  from the equilateral triangle  $(0, \sqrt{3}/2)$  is given by

$$R^2 = x^2 + (\sqrt{3}/2 - y)^2. \quad (3)$$

where

$$\begin{aligned} x &= (a^2 + b^2 - c^2)/(2a) - 1/2, \\ y &= 2S/a. \end{aligned} \quad (4)$$

Here,  $S$  is the area of the triangle, that is,  $S = \sqrt{s(s-a)(s-b)(s-c)}$  with  $s = (a+b+c)/2$ . If we put  $a = 1$ , we have instead of Eq. (4)

$$\begin{aligned} x &= (b^2 - c^2)/2, \\ y &= 2S. \end{aligned} \quad (5)$$

We want to know what happens to the shape if we approach the TCP from arbitrary directions. To see this, we numerically integrate orbits along the radial line centered at the TCP with azimuthal angles separated by  $60^\circ$  on the initial condition plane. We expect a similar tendency of the behaviors of the shape for different azimuthal angles, so we restrict to the azimuthal angles  $60^\circ$ ,  $120^\circ$ , and  $180^\circ$ . In addition, the behavior of the shape of the triangles formed by three bodies are expected similar near different TCPs. As a representative TCP, we choose (0.19208270, 0.30936018). For each azimuthal angle we choose

**Table 4** The initial conditions of orbit integration along the azimuthal directions  $60^\circ$ ,  $120^\circ$ , and  $180^\circ$  with distances 0.001, 0.0001, and 0.00001 from TCP: (0.19208270, 0.30936018).

radius: 0.001		
0.19258270	0.31022620	60.0
0.19158270	0.31022620	120.0
0.19108270	0.30936018	180.0
radius: 0.0001		
0.19213270	0.30944678	60.0
0.19203270	0.30944678	120.0
0.19198270	0.30936018	180.0
radius: 0.00001		
0.19208770	0.30936884	60.0
0.19207770	0.30936884	120.0
0.19207270	0.30936018	180.0

three radii,  $10^{-3}$ ,  $10^{-4}$  and  $10^{-5}$  at which orbit integrations are carried out. The positions and azimuthal directions are listed in Table 4.

We plot these directions relative to the BCCs in Fig. 5. BCCs are plotted with dots. In the figure, the TCP is represented by a filled circle. Three radii from the TCP are directed to the azimuthal angles  $60^\circ$ ,  $120^\circ$ , and  $180^\circ$ . These are above three BCCs. Remaining three directions would look downward. We omitted the orbit integrations along these three directions to avoid too much numerical data.

For the azimuthal angle  $60^\circ$ , we integrated orbits starting at distance  $10^{-3}$ ,  $10^{-4}$ , and  $10^{-5}$  from the TCP. For each orbit, we plotted the triangles formed by the three bodies at four or five instants just before the time of singularity of the triple collision orbit in order to see the change of the shape of the triangles with time. Figure 6 shows the results. There are simple tendencies. The shape of the triangles are not close to that of the equilateral triangle if the starting position is far away from the TCP (Fig. 6(a)). As the starting positions of the orbit approach the TCP (Figs. 6(b) and (c)), the shape of the triangles stay close to equilateral, and then at the final instants, it deviates from the equilateral shape. This can be confirmed looking at Fig. 6(d). In the figure, the ordinate represents the distance of the shape of the triangle from that of the equilateral triangle. The abscissa represents the time. Thus, the curve shows the change of the shape distance in time. As shown qualitatively in Figs. 6(a), (b), and (c), the orbits starting at distance 0.001 and 0.0001 from the TCP has the distance of the shape greater than 0.6 and 0.3, respectively, and increase the shape distance as the time proceeds, whereas the orbit starting at distance 0.00001 initially has the shape close to the equilateral triangle with the shape distance smaller than 0.05. Then it quickly increases the shape distance.

The above tendencies can be observed also in Figs. 7 and 8. These tendencies correspond to the behaviors of orbits near the triple collision manifold. The orbit of the real world, if it is not on the stable manifold of the triple

collision manifold, moves close to the orbit on the triple collision manifold and moves away from it, that is, the orbit approaches the triangular equilibrium point and moves away from it. In other words, the shape of the triangles formed by the three bodies becomes closer to the equilateral shape if the orbit is close to the triple collision orbit. This is what we observe in Figs. 6, 7 and 8. On the other hand, if the numerical calculation was infinitely precise and if one would be able to target the stable manifold of the triple collision, then the triangle would approach the equilateral shape. In this case, due to the time transformation, it would take an infinite time to arrive at triple collision.

In the case of the orbit off the stable manifold of the triple collision manifold, the shape of the triangle becomes closest to that of equilateral at some time and deviates from it as the orbit departs from triple collision manifold running closely along the unstable manifold of the triple collision manifold.

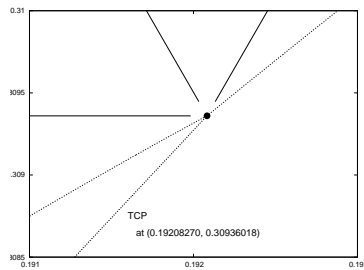


**Fig. 5** TCP at  $(0.19208270, 0.30936018)$  and three binary collision curves. The orbit integrations have been done along the radii  $60^\circ$ ,  $120^\circ$  and  $180^\circ$  centered at TCP.

## 5 Conclusion and Discussion

Now, we may answer the doubt proposed by Sergei Klioner. His doubt has been that ours may appear to be triple collision orbits due to the insufficient numerical accuracy.

It is true, as our numerical integrations of orbits in section 4 show, that the shape of the triangles of orbits formed by three bodies is close to equilateral until certain instants and deviates from it just before the time of supposed triple collision. Thus, our triple collision orbits may also change the shape of the triangle.

However, our numerical integrations of orbits in section 2 assures our results on the existence and discovery of TCPs (Tanikawa et al. 2019). In fact, the orbits starting at the positions on the BCCs experience binary collision at the supposed instant of triple collision. The shape of the triangle is of isosceles, and the base edge in the limit have a definite orientation. The orientations of

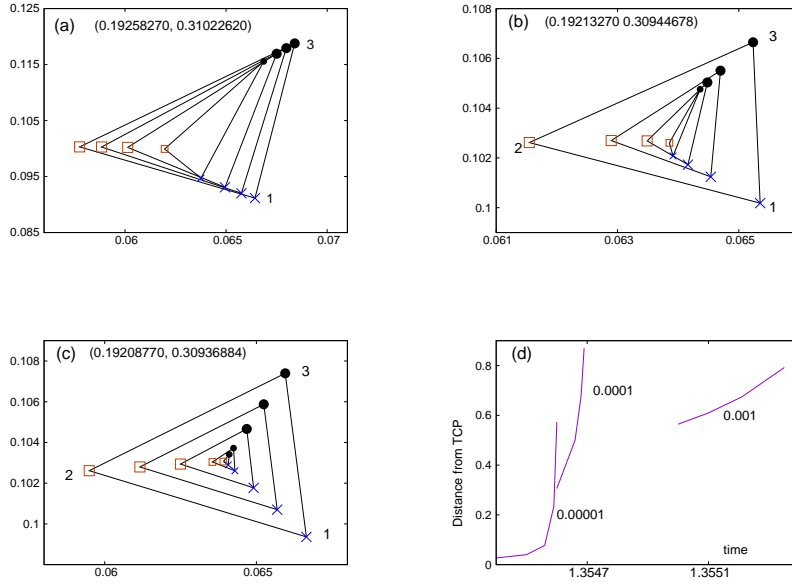


**Fig. 6** The evolution of the shape of the triangles formed by three bodies before the time of triple collision. The initial conditions of orbits are off the TCP.

the respective limiting orbits of the three BCCs form an equilateral triangle. In addition, the orientation of the equilateral triangle coincides with that of the triangle of our triple collision orbit, which ascertain that our TCPs are really TCPs.

The triple collision orbits we have obtained are all Lagrangian equilateral type. Three BCCs meet at a point on the initial condition plane  $D$ . Each curve determines the direction of bodies perpendicular to the base edge of the binary, hence the direction of the edge is determined. This direction represents one of the edges of the equilateral triangle. Thus, from our procedure, collinear triple collisions have been excluded.

Our triple collision orbits are actually ejection-collision orbits, that is, the orbits emerging at triple collision and ending at triple collision. Now we check the initial and final orientations of the triangles. Triangles are equilateral. Then what is the rotation angle?

The two dimensional configuration space is isotropic. The orientation of the equilateral triangle formed by three bodies is meaningful only when it is considered together with the orientation of the initial triangle formed by three bodies. For the time-being, Table 1 gives the poor data of characterization of the initial and final triangles including their orientations formed by three bodies.

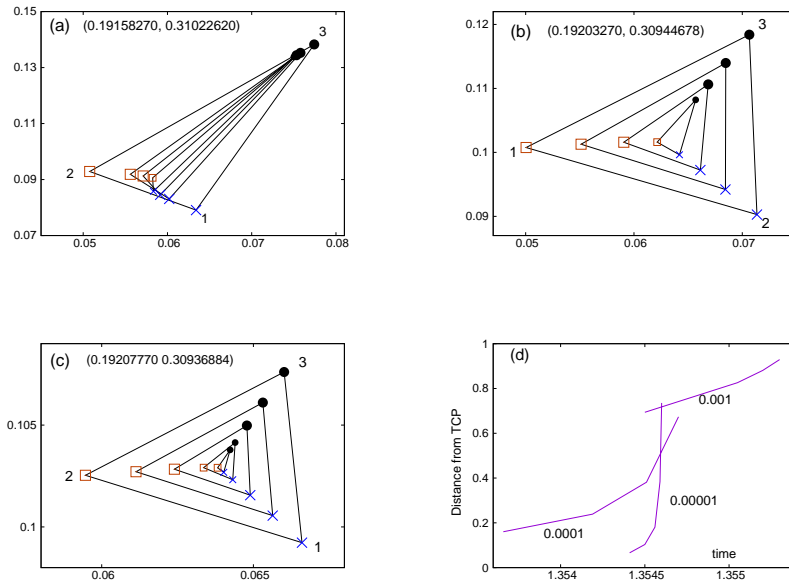


**Fig. 7** The evolution of the shape of the triangles formed by three bodies before the time of triple collision. The initial conditions of orbits are off the TCP.

We now understand that triple collision is characterized by the orientation of the final equilateral triangle (with respect to the initial orientation of the triangle). Then we expect that the number of triple collision orbits is not countable. The set of triple collision orbits has a cardinality of the continuum. In the equal-mass free-fall case, the number is countable. We have the freedom of continuously changing the mass of the three bodies, and also the freedom of continuously changing the initial velocities. This may give us an uncountable set of triple collisions.

## References

1. Robert L. Devaney; 1980, Triple collision in the planar isosceles three body problem, *Inventiones Mathematicae* **60**, 249-267.
2. McGehee, R.: 1974, Triple collision in the collinear three-body problem, *Inventiones Mathematicae* **27**, 191-227.
3. Mikkola, S. and Tanikawa, K.: 1999, Algorithmic regularization of the few-body problem *Mon. Not. R. Astronom. Soc.* **310**, 745 - 749.
4. Mikkola, S. and Tanikawa, K.: 2013, Implementation of an efficient logarithmic-Hamiltonian three-body code, *New Astronomy*, **20**, 38 - 41.
5. Moeckel, R.: 1989, Chaotic dynamics near triple collision, *Arch. Rat. Mech.* **107**, 37 - 68.
6. Montgomery, R.: 2007, The zero angular momentum three-body problem: all but one solution has syzygies. *Ergod. Theor. Dyn. Syst.* **27**, 1933-1946

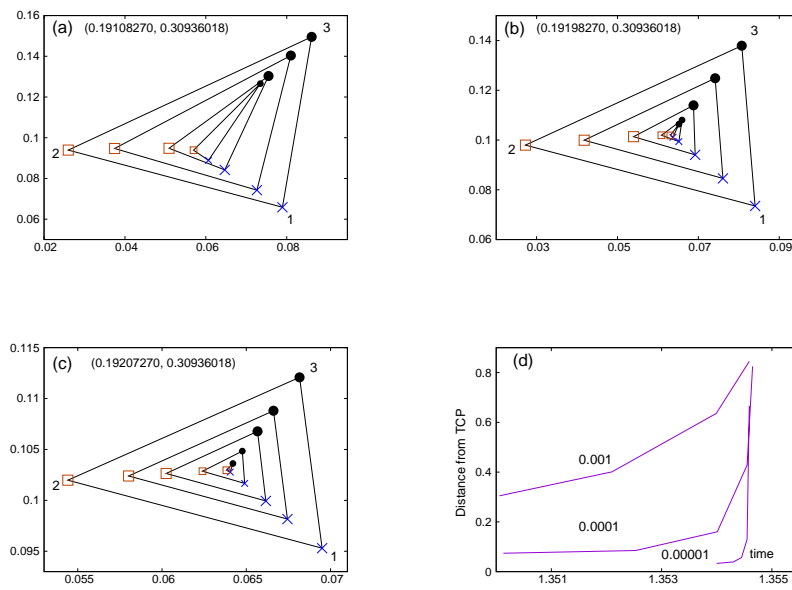


**Fig. 8** The evolution of the shape of the triangles formed by three bodies before the time of triple collision. The initial conditions of orbits are off the TCP.

7. Simó, C. and Martinez, R.: 1988 Qualitative study of the planar isosceles three-body problem, *Celestial Mechanics* **41**, 179-251
8. Tanikawa and Mikkola: 2015, Symbol sequences and orbits of the free-fall three-body problem, *Publ. Astron. Soc. Japan*, **67**, Issue 6, id.115 10 pp.
9. Tanikawa, K., Saito, M. M., and Mikkola, S. (Paper I): 2019, A search for triple collision orbits inside the domain of the free-fall three-body problem, *Cel. Mech. & Dyn. Astron.* **131**:24.
10. Zhihong Xia; 1992, The existence of noncollision singularities in newtonian systems *Annals of Mathematics* **135**, 411-468